arXiv:1303.4794v1 [physics.optics] 19 Mar 2013

Enhancing the near magnetic field with dielectric Mie resonators

Guillaume Boudarham,[1] Redha Abdeddaim,[1] Jean-Michel Geffrin,[1] and Nicolas Bonod[1,*]
[1] *Institut Fresnel, CNRS, Aix-Marseille Université, Ecole Centrale Marseille,*
Campus Universitaire de Saint Jérôme, 13013 Marseille, France

(Dated: March 21, 2013)

Dielectric Mie resonators of moderate dielectric permittivity $\epsilon \approx 16$ are used to enhance the near magnetic field. Experiments are carried out in the GHz spectral regime with dielectric cubes of subwavelength size. The dielectric permittivity chosen in this experiment mimicks that of semiconductor materials such as silicon or gallium arsenide in the optical and near infrared regime so that the results presented in this Letter can be extended to a broad spectrum. By coupling two identical cubes, we are able to measure magnetic field intensities enhanced by two orders of magnitude. Experiments are completed with a general model able to predict with a high accuracy both electric and magnetic field intensities between neighboring Mie resonators.

Artifical magnetism is considered as one of the major breakhrought of modern photonics since it opened the way towards resonant magnetic light matter interactions. By suitably designing metallic particles at a scale much smaller than the incident wavelength, it is possible to create artificial meta-atoms that exhibit large electric and magnetic polarization moments when excited by an electromagnetic field. Split ring resonators or U-sphaped particles are the emblems of such artifical magneto-electric meta-atoms [1–5], even if more recently inverse antennas also proved their ability to create strong magnetic fields [6, 7]. Besides metallic nanostructures, high dielectric permittivity (typically much larger than 10) resonators supporting Mie resonances can also resonantly interact with incident electromagnetic field via electric or magnetic photonic modes [8]. The main interest of lossy materials is that they exhibit modes with high quality [9, 10]. But if materials exhibiting high refractive index can be easily found in THz and GHz spectral regions with ferroelectric and polaritonic materials, such materials suffer from high losses in the optical or near-infrared spectral regime that spoil the Mie resonances. More recently, materials of moderate dielectric permittivity (typically around 12) such as semi-conductors in the near-infrared and optical frequencies were showed to exhibit electric and magnetic Mie resonances of good quality [11]. The first experimental evidence of artificial magnetism with dielectric particles in the optical regime was carried out with silicon particles obtained with laser ablation [12]. The resonant magnetic and electric polarization of such particles leads to very intringuing far field scattering properties. In particular, such particles can satisfy the so-called Kerker's conditions originally predicted in 1983 for magnetic spheres to control the backward or forward scattering of light [13–15]. The first experimental observation was carried out recently in the GHz regime [16] and lastly at optical frequencies with silicon and gallium arsenide particles [17, 18].

In this Letter, we propose to investigate the near field properties of lossless Mie resonators with a special interest to the magnetic field enhancement. We propose to take benefit of the property featured by the magnetic field to be parallel to the substrate interface to investigate the hybridization of magnetic modes between neighboring particles. We present an experiment set-up able to measure the enhancement of the magnetic field intensity inside the gap of the dielectric dimer antenna [19]. The experimental measurements are carried out in the GHz regime with dielectric resonators of cubic shape. The constitutive material of the resonators (Eccostock HIK, K=16) exhibits a dielectric permittivity of 16 which is close to the dielectric permittivities offered by semiconductors in the optical or near-infrared regime. Consequently, the results demonstrated in this study can be extended to a very large spectrum ranging from optical to radio-frequencies. The experimental measurements were made in an anechoic chamber. The illumination is made through a horn antenna (1-18 GHz) and the measurement of the magnetic field is carried out with a high resolution near-field probe (1-6 GHz).

We first consider an individual dielectric cube with length $L = 16\,mm$ and permittivity $\epsilon \approx 16$ embedded in air and illuminated in normal incidence by a plane wave $(\boldsymbol{E}_0, \boldsymbol{H}_0)$, where $\boldsymbol{E}_0$ and $\boldsymbol{H}_0$ respectively denote the incident electric and magnetic fields [see Fig. 1 (a)]. Fig. 1 (b) (blue line) shows the normalized magnetic intensity $|\boldsymbol{H}|^2/|\boldsymbol{H}_0|^2$ ($\boldsymbol{H}$ being the total magnetic field) measured as a function of frequency when the probe is located at 1 mm from the center of the cube face, in the direction of the incident magnetic field. One can see that the enhancement of the magnetic intensity is maximal at 3.69 GHz where it reaches 60. The corresponding wavelength equal to 8 cm is much larger than the caracteristic size of the cube. It can be assumed at this stage that this enhancement is due to the excitation of a magnetic dipolar resonance of the cube, which will be confirmed later in Fig. 2 (a).

We propose to further increase the magnetic intensity enhancement by coupling a second cube, strictly iden-

---

* nicolas.bonod@fresnel.fr

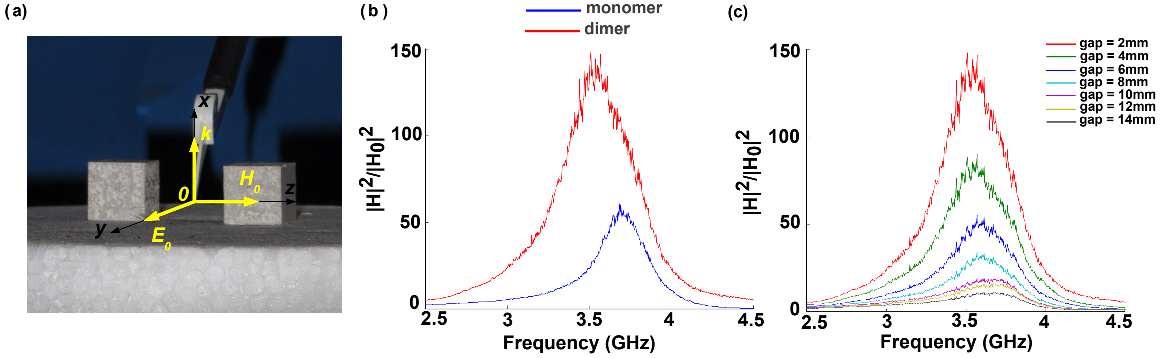

Figure 1. (Color online) (a) Photography of the experimental setup with the cartesian coordinates used in this study. The probe is visible between the cubes. (b) Normalized magnetic intensity as a function of frequency when the probe is located at 1 mm from the center of the cube face (blue line) compared to that obtained in the center of a dimer of cubes with a gap size of 2 mm (red line). (c) Normalized magnetic intensity as a function of frequency and gap size measured in the center of the dimer.

tical to the first. The two neighboring resonators are separated by a gap varying from 2 mm to 16 mm. This dielectric dimer antenna is then illuminated in normal incidence with an incident magnetic field parallel to the dimer axis : $\boldsymbol{H}_0 || \hat{\boldsymbol{z}}$ [see Fig. 1 (a)]. This condition of illumination allows for a maximal coupling of the magnetic modes supported by the neighboring cubes. Fig. 1 (b) (red line) shows the enhancement obtained for a gap size of 2 mm with respect to the illuminating frequency. The maximum enhancement reaches now 141 at 3.54 GHz, which is almost twice larger than the enhancement already measured with a single Mie resonator at the same position of the probe. Furthermore, due to the coupling between the two magnetic modes, the spectral position of the maximal enhancement obtained with the dimer is slightly redshifted compared to that obtained with a monomer.

Fig. 1 (c) shows the normalized magnetic intensity measured in the center of the dimer as a function of both frequency and gap size (see also the supplemental material). As expected, we see that the magnetic enhancement increases as the gap size decreases, which will be confirmed later theoretically. We also observe the effect of the coupling on the spectral position of the maximum enhancement. As it is observed by using metallic dimer antennas with electric field intensity when the incident electric field is polarized along the dimer axis [20], hybridization of magnetic modes leads to a redshift of the resonance.

We now derive below a general effective polarizability model to calculate semi-analytically the magnetic intensity enhancement measured experimentally inside the gap of the dimer. We use the international system of units and for simplification, we will take $|\boldsymbol{E}_0| = 1$ and thus $|\boldsymbol{H}_0| = 1/Z_0$, where $Z_0 = 376.730\,\Omega$ is the impedance of free space [21] and we will not explicitly indicate the frequency dependence of the quantities introduced.

The length of the cube is around a tenth of the illuminating wavelength at resonance, which leads us to perform the analytic derivation under a dipolar approximation. A particle n $(n = 1, 2)$ of the dimer located at $\boldsymbol{r}_n$ is assumed to respond with an induced electric and magnetic dipole respectively noted $\boldsymbol{p}_n$ and $\boldsymbol{m}_n$. The electric and magnetic dipoles of each particle, that we assume here identical and non-bianisotropic and described by the polarizability tensor $\bar{\bar{\boldsymbol{\alpha}}} = \mathrm{diag}(\bar{\bar{\boldsymbol{\alpha}}}_e, \bar{\bar{\boldsymbol{\alpha}}}_m)$, where $\bar{\bar{\boldsymbol{\alpha}}}_e$ and $\bar{\bar{\boldsymbol{\alpha}}}_m$ respectively denote the electric and magnetic polarizability tensors of the particles, verify the general tensorial system of equations [22]

$$\begin{pmatrix} \boldsymbol{p}_n/\epsilon_0 \\ \boldsymbol{m}_n \end{pmatrix} = \bar{\bar{\boldsymbol{\alpha}}}\cdot \left[\begin{pmatrix} \boldsymbol{E}_0(\boldsymbol{r}_n) \\ \boldsymbol{H}_0(\boldsymbol{r}_n) \end{pmatrix} + \sum_{\substack{q=1,2 \\ q\neq n}} \bar{\bar{\boldsymbol{G}}}^0(\boldsymbol{r}_n, \boldsymbol{r}_q) \cdot \begin{pmatrix} \boldsymbol{p}_q \\ \boldsymbol{m}_q \end{pmatrix} \right], \tag{1}$$

where

$$\bar{\bar{\boldsymbol{G}}}^0(\boldsymbol{r}, \boldsymbol{r}') = \begin{pmatrix} \bar{\bar{\boldsymbol{G}}}^0_{ee}(\boldsymbol{r}, \boldsymbol{r}') & \bar{\bar{\boldsymbol{G}}}^0_{em}(\boldsymbol{r}, \boldsymbol{r}') \\ \bar{\bar{\boldsymbol{G}}}^0_{me}(\boldsymbol{r}, \boldsymbol{r}') & \bar{\bar{\boldsymbol{G}}}^0_{mm}(\boldsymbol{r}, \boldsymbol{r}') \end{pmatrix} \tag{2}$$

is the dyadic Green's function of free space. The 3×3 diagonal blocks correspond to the well-known electric and magnetic dyadic Green's functions of free space [23]. The off-diagonal blocks correspond to the mixed dyadics that give the electric field at $\boldsymbol{r}$ due to a magnetic dipole at $\boldsymbol{r}'$ and the magnetic field at $\boldsymbol{r}$ due to an electric dipole at $\boldsymbol{r}'$. $\boldsymbol{E}_0(\boldsymbol{r}_n)$ and $\boldsymbol{H}_0(\boldsymbol{r}_n)$ respectively denote the incident electric and magnetic fields at $\boldsymbol{r}_n$. The second term inside the brackets represents the field scattered by the other particle and $\epsilon_0 = 1/\mu_0 c^2 = 8.85.10^{-12}\,F.m^{-1}$ is the permittivity of free space, where $\mu_0 = 4\pi 10^{-7} T.m.A^{-1}$ is the permeability of free space and c is the velocity of light. In the following, we assume that the incident wavevector is transverse to the dimer axis : $\boldsymbol{k}||\hat{\boldsymbol{x}}$ [see Fig. 1 (a)], then the dipolar moments of each particle are excited in phase and by assuming a non-zero but weak magneto-electric coupling between the particles : $\boldsymbol{p}_1 = \boldsymbol{p}_2 \equiv \boldsymbol{p}$ and $\boldsymbol{m}_1 = \boldsymbol{m}_2 \equiv \boldsymbol{m}$. From Eq. (1), we obtain

$$\boldsymbol{p} = \epsilon_0 \bar{\bar{\boldsymbol{\alpha}}}_e \cdot \left[\boldsymbol{E}_0 + \bar{\bar{\boldsymbol{G}}}^0_{ee} \cdot \boldsymbol{p} + \bar{\bar{\boldsymbol{G}}}^0_{em} \cdot \boldsymbol{m} \right] \quad (3)$$

$$\boldsymbol{m} = \bar{\bar{\boldsymbol{\alpha}}}_m \cdot \left[\boldsymbol{H}_0 + \bar{\bar{\boldsymbol{G}}}^0_{me} \cdot \boldsymbol{p} + \bar{\bar{\boldsymbol{G}}}^0_{mm} \cdot \boldsymbol{m} \right], \quad (4)$$

where we have noted $\boldsymbol{E}_0(\boldsymbol{r}_1) = \boldsymbol{E}_0(\boldsymbol{r}_2) \equiv \boldsymbol{E}_0$ and $\boldsymbol{H}_0(\boldsymbol{r}_1) = \boldsymbol{H}_0(\boldsymbol{r}_2) \equiv \boldsymbol{H}_0$. Substituting in Eq. (3) the expression of $\boldsymbol{m}$ written in terms of $\boldsymbol{p}$ obtained from Eq. (4), we obtain the expression of $\boldsymbol{p}$ in terms of $\boldsymbol{E}_0$ and $\boldsymbol{H}_0$. Now substituting the previous expression in Eq. (4), we get the expression of $\boldsymbol{m}$ in terms of $\boldsymbol{E}_0$ and $\boldsymbol{H}_0$. Finally, $\boldsymbol{p}$ and $\boldsymbol{m}$ can be cast

$$\boldsymbol{p}/\epsilon_0 = \bar{\bar{\boldsymbol{\alpha}}}^{\mathrm{eff}}_{ee} \cdot \boldsymbol{E}_0 + Z_0 \bar{\bar{\boldsymbol{\alpha}}}^{\mathrm{eff}}_{em} \cdot \boldsymbol{H}_0 \quad (5)$$

$$\boldsymbol{m} Z_0 = Z_0 \bar{\bar{\boldsymbol{\alpha}}}^{\mathrm{eff}}_{mm} \cdot \boldsymbol{H}_0 + \bar{\bar{\boldsymbol{\alpha}}}^{\mathrm{eff}}_{me} \cdot \boldsymbol{E}_0, \quad (6)$$

where we have introduced the effective polarizabilities $\bar{\bar{\boldsymbol{\alpha}}}^{\mathrm{eff}}_{ee}$, $\bar{\bar{\boldsymbol{\alpha}}}^{\mathrm{eff}}_{mm}$, $\bar{\bar{\boldsymbol{\alpha}}}^{\mathrm{eff}}_{em}$ and $\bar{\bar{\boldsymbol{\alpha}}}^{\mathrm{eff}}_{me}$:

$$\bar{\bar{\boldsymbol{\alpha}}}^{\mathrm{eff}}_{ee} = \bar{\bar{\boldsymbol{T}}}_e \cdot \bar{\bar{\boldsymbol{\alpha}}}_e \quad (7)$$

$$\bar{\bar{\boldsymbol{\alpha}}}^{\mathrm{eff}}_{mm} = \bar{\bar{\boldsymbol{T}}}_m \cdot \bar{\bar{\boldsymbol{\alpha}}}_m \quad (8)$$

$$\bar{\bar{\boldsymbol{\alpha}}}^{\mathrm{eff}}_{em} = \frac{1}{Z_0} \bar{\bar{\boldsymbol{T}}}_e \cdot \bar{\bar{\boldsymbol{\alpha}}}_e \cdot \bar{\bar{\boldsymbol{G}}}^0_{em} \cdot [\bar{\bar{\boldsymbol{I}}} - \bar{\bar{\boldsymbol{\Gamma}}}_m]^{-1} \cdot \bar{\bar{\boldsymbol{\alpha}}}_m \quad (9)$$

$$\bar{\bar{\boldsymbol{\alpha}}}^{\mathrm{eff}}_{me} = \epsilon_0 Z_0 \bar{\bar{\boldsymbol{T}}}_m \cdot \bar{\bar{\boldsymbol{\alpha}}}_m \cdot \bar{\bar{\boldsymbol{G}}}^0_{me} \cdot [\bar{\bar{\boldsymbol{I}}} - \bar{\bar{\boldsymbol{\Gamma}}}_e]^{-1} \cdot \bar{\bar{\boldsymbol{\alpha}}}_e, \quad (10)$$

with

$$\bar{\bar{\boldsymbol{T}}}_e = [\bar{\bar{\boldsymbol{I}}} - \bar{\bar{\boldsymbol{\Gamma}}}_e - \bar{\bar{\boldsymbol{\Gamma}}}_{em}]^{-1} \quad (11)$$

$$\bar{\bar{\boldsymbol{T}}}_m = [\bar{\bar{\boldsymbol{I}}} - \bar{\bar{\boldsymbol{\Gamma}}}_m - \bar{\bar{\boldsymbol{\Gamma}}}_{me}]^{-1} \quad (12)$$

and

$$\bar{\bar{\boldsymbol{\Gamma}}}_e = \epsilon_0 \bar{\bar{\boldsymbol{\alpha}}}_e \cdot \bar{\bar{\boldsymbol{G}}}^0_{ee} \quad (13)$$

$$\bar{\bar{\boldsymbol{\Gamma}}}_m = \bar{\bar{\boldsymbol{\alpha}}}_m \cdot \bar{\bar{\boldsymbol{G}}}^0_{mm} \quad (14)$$

$$\bar{\bar{\boldsymbol{\Gamma}}}_{em} = \epsilon_0 \bar{\bar{\boldsymbol{\alpha}}}_e \cdot \bar{\bar{\boldsymbol{G}}}^0_{em} \cdot [\bar{\bar{\boldsymbol{I}}} - \bar{\bar{\boldsymbol{\alpha}}}_m \cdot \bar{\bar{\boldsymbol{G}}}^0_{mm}]^{-1} \cdot \bar{\bar{\boldsymbol{\alpha}}}_m \cdot \bar{\bar{\boldsymbol{G}}}^0_{me} \quad (15)$$

$$\bar{\bar{\boldsymbol{\Gamma}}}_{me} = \epsilon_0 \bar{\bar{\boldsymbol{\alpha}}}_m \cdot \bar{\bar{\boldsymbol{G}}}^0_{me} \cdot [\bar{\bar{\boldsymbol{I}}} - \epsilon_0 \bar{\bar{\boldsymbol{\alpha}}}_e \cdot \bar{\bar{\boldsymbol{G}}}^0_{ee}]^{-1} \cdot \bar{\bar{\boldsymbol{\alpha}}}_e \cdot \bar{\bar{\boldsymbol{G}}}^0_{em}, \quad (16)$$

where $\bar{\bar{\boldsymbol{I}}} = \mathrm{diag}(1,1,1)$ denotes the 3 × 3 matrix identity. As expected, the coupled resonators exhibit dipolar moments similar to those observed with bianisotropic particles.

For simplification, the dimer axis is taken along the z-axis of the coordinate system. In these conditions, only certain elements of the dyadic Green's functions are non null. See the Supplemental material for the explicit expressions of the Green's function elements. Given the symmetry of the particles considered here, the electric and magnetic polarizability tensors are diagonal and can be described with scalars : $\bar{\bar{\boldsymbol{\alpha}}}_e = \alpha_e \mathrm{diag}(1,1,1)$ and $\bar{\bar{\boldsymbol{\alpha}}}_m = \alpha_m \mathrm{diag}(1,1,1)$, where : $\alpha_e \equiv \alpha^{yy}_{ee} = p_y/\epsilon_0$ and $\alpha_m \equiv \alpha^{zz}_{mm} = m_z Z_0$ [21] and by assuming that the isolated cube is illuminated by a plane wave such as $\boldsymbol{H}_0 || \hat{\boldsymbol{z}}$ and $\boldsymbol{E}_0 || \hat{\boldsymbol{y}}$. Therefore α_e and α_m can be deduced from the knowledge of $\boldsymbol{p}$ and $\boldsymbol{m}$ that we obtained by calculating the polarization density $\boldsymbol{P}$ with a Finite Element Method implemented in COMSOL Multiphysics : $\boldsymbol{p} = \int \boldsymbol{P} d^3\boldsymbol{r}$ and $\boldsymbol{m} = -j\omega/2 \int \boldsymbol{r} \times \boldsymbol{P} d^3\boldsymbol{r}$, where the integration is performed over the volume of the structure [21]. After some algebraic manipulations, the expressions (13)-(16) can be cast

$$\bar{\bar{\boldsymbol{\Gamma}}}_e = \epsilon_0 \alpha_e \begin{pmatrix} G^0_{ee,xx} & 0 & 0 \\ 0 & G^0_{ee,yy} & 0 \\ 0 & 0 & G^0_{ee,zz} \end{pmatrix} \quad (17)$$

$$\bar{\bar{\boldsymbol{\Gamma}}}_m = \alpha_m \begin{pmatrix} G^0_{mm,xx} & 0 & 0 \\ 0 & G^0_{mm,yy} & 0 \\ 0 & 0 & G^0_{mm,zz} \end{pmatrix} \quad (18)$$

$$\bar{\bar{\boldsymbol{\Gamma}}}_{em} = \epsilon_0 \alpha_e \alpha_m \frac{G^0_{em,xy} G^0_{me,yx}}{1 - \alpha_m G^0_{mm,yy}} \begin{pmatrix} 1 & 0 & 0 \\ 0 & 1 & 0 \\ 0 & 0 & 0 \end{pmatrix} \quad (19)$$

$$\bar{\bar{\boldsymbol{\Gamma}}}_{me} = \epsilon_0 \alpha_e \alpha_m \frac{G^0_{me,xy} G^0_{em,yx}}{1 - \epsilon_0 \alpha_e G^0_{ee,yy}} \begin{pmatrix} 1 & 0 & 0 \\ 0 & 1 & 0 \\ 0 & 0 & 0 \end{pmatrix}. \quad (20)$$

Expressions (5) and (6) now give

$$\boldsymbol{p} = \frac{\epsilon_0 \alpha_e |\boldsymbol{E}_0| \hat{\boldsymbol{e}}_y}{1 - \gamma_T - \gamma_{TL}} \quad (21a)$$

$$\boldsymbol{m} = \frac{\alpha_m |\boldsymbol{H}_0| \hat{\boldsymbol{e}}_z}{1 - \gamma_L} + \frac{\gamma_{TL} |\boldsymbol{E}_0| \hat{\boldsymbol{e}}_x}{(1 - \gamma_T - \gamma_{TL}) G^0_{em,yx}}, \quad (21b)$$

where

$$\gamma_T \equiv \epsilon_0 \alpha_e G^0_{ee,yy}, \quad \gamma_L \equiv \alpha_m G^0_{mm,zz} \quad (22)$$

$$\gamma_{TL} \equiv \epsilon_0 \alpha_e \alpha_m \frac{G^0_{em,yx} G^0_{me,xy}}{1 - \alpha_m G^0_{mm,xx}}. \quad (23)$$

γ_T and γ_L represent the transverse and longitudinal interparticle scattering for the electric and magnetic field respectively. γ_T and γ_L take into account the electric and magnetic field scattered in one particle by the electric and magnetic dipolar moments of the other particle respectively. γ_{TL} is a cross-coupling term which takes into account the magnetic field scattered in one particle by the electric dipolar moment of the other particle.

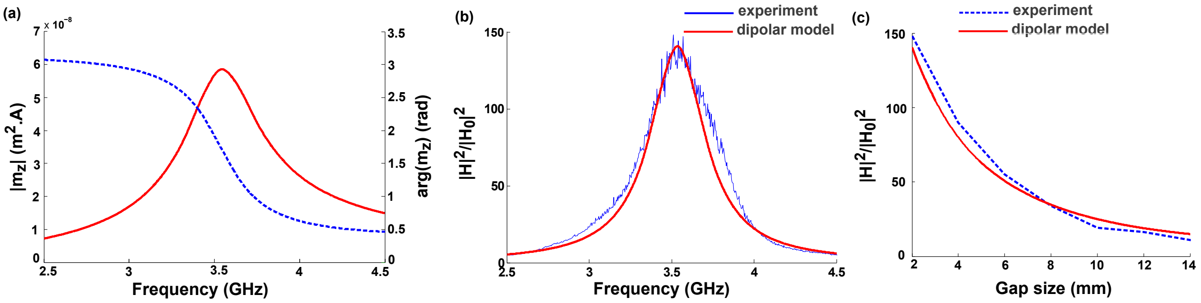

Figure 2. (Color online) (a) Modulus (full red line, left scale) and phase (dashed blue line, right scale) of the magnetic dipolar moment m_z of each cube obtained from Eq. (21b) for a dimer with a gap size of 2 mm. (b) Normalized magnetic intensity in the center of the dimer with a gap size of 2 mm as a function of frequency obtained with the dipolar model (red line), compared to experimental measurements (blue line). (c) Maximum value of the normalized magnetic intensity in the center of the dimer as a function of gap size obtained with the dipolar model (red line), compared to experimental measurements (dashed blue line).

Eqs. (5) and (6) evidence that each particle coupled to the other behaves as if it were bianisotropic while the individual particle is assumed non-bianisotropic. This can be explained by the fact that the incident magnetic field excites the magnetic dipole of one particle which induces an electric field on the other particle and excites the electric dipole, and vice versa. This effect is respectively described by the effective polarizabilities $\bar{\bar{\boldsymbol{\alpha}}}_{em}^{\mathrm{eff}}$ and $\bar{\bar{\boldsymbol{\alpha}}}_{me}^{\mathrm{eff}}$. We note also that due to the illumination conditions used in this work, the electric dipolar moment $\boldsymbol{p}$ does no longer depends on the incident magnetic field [see Eq. (21a)]. Moreover, the cross-coupling term implies that the direction of the magnetic dipolar moment $\boldsymbol{m}$ does not coincide with the direction of the incident magnetic field (z-axis), while the electric dipolar moment $\boldsymbol{p}$ remains parallel to the incident electric field (y-axis).

Fig. 2 (a) shows the magnetic dipolar moment m_z obtained from the dipolar model [see Eq. (21b)] for a gap size of 2 mm. The maximum of the modulus together with a phase value close to $\pi/2$ at 3.54 GHz is characteristic of a resonance. This frequency is very close to that of the maximum enhancement in Fig. 1 (b) (red line). It is therefore obvious that this enhancement is caused by the resonant excitation of the magnetic dipole resonance (aligned with the z-axis) of the cubes. Fig. 2 (b) shows the normalized magnetic intensity in the center of the gap of the dimer as a function of frequency obtained from the dipolar model (red line) and compared to the experimental measurement (blue line). The red curve has been obtained by calculating the magnetic field inside the gap created by two magnetic dipoles m_z oriented along z and centered in each cube [21]

$$H_z = 2G^0_{mm,zz} m_z = [2e^{jkl}(1-jkl)/2\pi l^3] m_z, \qquad (24)$$

where l is the distance between the center of one cube and the center of the gap and m_z is given by Eq. (21b). Otherwise, the contribution to the magnetic field inside the gap due to the electric dipoles p_y of each cube is zero by symmetry and is not taken into account. The dipolar model derived in this Letter shows a remarkable agreement with experiments. The previous expression of H_z also shows that the normalized magnetic intensity $|\boldsymbol{H}|^2/|\boldsymbol{H}_0|^2$ is varying roughly as $1/l^6 + k^2/l^4$ meaning that it increases as the distance l decreases which is in good agreement with the experimental measurements [see Fig. 2 (c)]. This result implies also that it is possible to obtain a magnetic enhancement more important than that obtained with a gap size of 2 mm even further reducing the distance between the cubes. In summary, dielectric Mie resonators appear as ideal devices to enhance the near magnetic field. By coupling two identical resonators, we measured experimentally magnetic field intensities enhanced by two orders of magnitude. This enhancement is allowed by the coupling of the magnetic moments parallel to the dimer axis. Experimental investigations were completed by a detailed analytical model that is able to predict with a high accuracy the magnetic field intensity with respect to the dipolar moments of the resonators, the illuminating wavelength and the length of the gap. This model is very general and could also be applied to other illuminating configurations and also to the calculation of the electric field. Finally, the results presented in this Letter in the microwave domain can be extended to other spectral domains since they were obtained with a material exhibiting a dielectric permittivity that can be observed in a very broad spectrum ranging from optics to radio-frequencies.

ACKNOWLEDGMENTS

The authors would like to thank Sebastien Bidault and Elodie Georget for their interest and helpfull discussions. This research was funded by the French Agence Nationale de la Recherche under Contract No. ANR-11-BS10-002-02 TWINS.

---

[1] C. Enkrich, M. Wegener, S. Linden, S. Burger, L. Zschiedrich, F. Schmidt, J. F. Zhou, T. Koschny, and M. Soukoulis, C., Phys. Rev. Lett. **95**, 203901 (Nov. 2005)

[2] C. Rockstuhl, T. Zentgraf, E. Pshenay-Severin, J. Petschulat, A. Chipouline, J. Kuhl, T. Pertsch, H. Giessen, and F. Lederer, Opt. Express **15**, 8871 (Jul 2007), `http://www.opticsexpress.org/abstract.cfm?URI=oe-15-14-8871`

[3] M. W. Klein, C. Enkrich, M. Wegener, C. M. Soukoulis, and S. Linden, Opt. Lett. **31**, 1259 (May 2006), `http://ol.osa.org/abstract.cfm?URI=ol-31-9-1259`

[4] M. Husnik, M. W. Klein, N. Feth, M. König, J. Niegemann, K. Busch, S. Linden, and M. Wegener, Nature Photonics **2**, 614 (2008)

[5] I. Sersic, C. Tuambilangana, T. Kampfrath, and A. F. Koenderink, Phys. Rev. B: Condens. Matter Mater. Phys. **83**, 245102 (Jun 2011), `http://link.aps.org/doi/10.1103/PhysRevB.83.245102`

[6] T. Grosjean, M. Mivelle, F. I. Baida, G. W. Burr, and U. C. Fischer, Nano Letters **11**, 1009 (2011)

[7] H. Kihm, S. Koo, Q. Kim, K. Bao, J. Kihm, W. Bak, S. Eah, C. Lienau, H. Kim, P. Nordlander, *et al.*, Nature Communications **2**, 451 (2011)

[8] F. Zhang, L. Kang, Q. Zhao, J. Zhou, and D. Lippens, New Journal of Physics **14**, 033031 (2012)

[9] J. A. Schuller, R. Zia, T. Taubner, and M. L. Brongersma, Physical Review Letters **99**, 107401 (Sep 2007), `http://link.aps.org/doi/10.1103/PhysRevLett.99.107401`

[10] Q. Zhao, J. Zhou, F. Zhang, and D. Lippens, Materials Today **12**, 60 (Dec. 2009), `http://dx.doi.org/10.1016/S1369-7021(09)70318-9`

[11] A. García-Etxarri, R. Gómez-Medina, L. S. Froufe-Pérez, C. López, L. Chantada, F. Scheffold, J. Aizpurua, M. Nieto-Vesperinas, and J. J. Sáenz, Optics Express **19**, 4815 (Mar 2011), `http://www.opticsexpress.org/abstract.cfm?URI=oe-19-6-4815`

[12] A. B. Evlyukhin, S. M. Novikov, U. Zywietz, R. L. Eriksen, C. Reinhardt, S. I. Bozhevolnyi, and B. N. Chichkov, Nano Letters **12**, 3749 (2012)

[13] M. Kerker, D.-S. Wang, and C. L. Giles, Journal of the Optical Society of America **73**, 765 (Jun 1983), `http://www.opticsinfobase.org/abstract.cfm?URI=josa-73-6-765`

[14] R. Gomez-Medina, B. Garcia-Camara, I. Suarez-Lacalle, F. Gonzalez, F. Moreno, M. Nieto-Vesperinas, and J. J. Saenz, Journal of Nanophotonics **5**, 053512 (2011), `http://link.aip.org/link/?JNP/5/053512/1`

[15] B. Rolly, B. Stout, and N. Bonod, Optics Express **20**, 20376 (Aug 2012), `http://www.opticsexpress.org/abstract.cfm?URI=oe-20-18-20376`

[16] J. Geffrin, B. García-Cámara, R. Gómez-Medina, P. Albella, L. Froufe-Pérez, C. Eyraud, A. Litman, R. Vaillon, F. González, M. Nieto-Vesperinas, *et al.*, Nature communications **3**, 1171 (2012)

[17] S. Person, M. Jain, Z. Lapin, J. J. Saenz, G. Wicks, and L. Novotny, Nano Letters, in press(2013)

[18] Y. H. Fu, A. I. Kuznetsov, A. E. Miroshnichenko, Y. F. Yu, and B. Lukyanchuk, Nature Communications **4**, 1527 (2013)

[19] B. Rolly, B. Bebey, S. Bidault, B. Stout, and N. Bonod, Physical Review B: Condensed Matter and Materials Physics **85**, 245432 (Jun 2012), `http://link.aps.org/doi/10.1103/PhysRevB.85.245432`

[20] G. Li, X. Chen, L. Huang, J. Wang, W. Hu, and W. Lu, Physica B: Condensed Matter(2012)

[21] J. D. Jackson, *Classical Electrodynamics : Third Edition* (John Wiley & Sons, New York, 1999) `http://books.google.fr/books?id=U3LBQgAACAAJ`

[22] F. G. De Abajo, Reviews of modern physics **79**, 1267 (2007)

[23] L. Novotny and B. Hecht, *Principles of Nano-Optics* (Cambridge University Press, 2006) `http://books.google.fr/books?id=Qrf036kThTQC`